Ruthenium Complexes for 1- and 2-Photon Photodynamic Therapy: From *In Silico* Prediction to *In Vivo* Applications

Johannes Karges[a], Shi Kuang[b], Federica Maschietto[c], Olivier Blacque[d], Ilaria Ciofini[c], Hui Chao[b,] and Gilles Gasser[a,*]*

[a] Chimie ParisTech, PSL University, CNRS, Institute of Chemistry for Life and Health Sciences, Laboratory for Inorganic Chemical Biology, 75005 Paris, France.

[b] MOE Key Laboratory of Bioinorganic and Synthetic Chemistry, School of Chemistry, Sun Yat-sen University, 510275 Guangzhou, People's Republic of China.

[c] Chimie ParisTech, PSL University, CNRS, Institute of Chemistry for Life and Health Sciences, Theoretical Chemistry and Modelling, 75005 Paris, France.

[d] Department of Chemistry, University of Zurich, Winterthurerstrasse 190, CH-8057, Zurich, Switzerland.

*Email: ceschh@mail.sysu.edu.cn, Tel. +86 2084110613, Email: gilles.gasser@chimieparistech.psl.eu; Tel. +33 144275602.

ORCID-ID:

Johannes Karges: 0000-0001-5258-0260

Shi Kuang: 0000-0003-3520-9499

Federica Maschietto: 0000-0002-5995-2765

Olivier Blacque: 0000-0001-9857-4042

Ilaria Ciofini: 0000-0002-5391-4522

Hui Chao: 0000-0003-4153-5303

Gilles Gasser: 0000-0002-4244-5097

Keywords: Anticancer, Medicinal Inorganic Chemistry, Metals in Medicine, Photosensitiser; Photodynamic Therapy.

ABSTRACT

The use of photodynamic therapy (PDT) against cancer has received increasing attention over the recent years. However, the application of the currently approved photosensitizers (PSs) is somehow limited by their poor aqueous solubility, aggregation, photobleaching and slow clearance from the body. To overcome these limitations, there is a need for the development of new classes of PSs with ruthenium(II) polypyridine complexes currently gaining momentum. However, these compounds generally lack significant absorption in the biological spectral window, limiting their application to treat deep-seated or large tumors. To overcome this drawback, ruthenium(II) polypyridine complexes designed *in silico* with (*E*,*E*')-4,4′-bisstyryl-2,2′-bipyridine ligands showed impressive 1- and 2-Photon absorption up to a magnitude higher than the ones published so far. While non-toxic in the dark, these compounds were found phototoxic in various 2D monolayer cells, 3D multicellular tumor spheroids and be able to eradicate a multiresistant tumor inside a mouse model upon clinically relevant 1-Photon and 2-Photon excitation.

INTRODUCTION

Due to an increasing impact of cancer on the life quality and mortality of human, increasing research efforts are devoted towards the development of novel anticancer drugs and strategies. Among the most commonly used techniques to fight this disease (i.e., surgery, chemotherapy and radiotherapy), photodynamic therapy (PDT) has received increasing attention during the last decades. In PDT, a photosensitizer (PS) is activated upon light irradiation to generate reactive oxygen species (ROS).[1-2] As the majority of currently approved photosensitizers (PSs) are based on tetrapyrrolic structures (i.e., porphyrin, chlorin, phthalocyanine), these compounds share similar drawbacks (e.g., poor aqueous solubility, aggregation, photobleaching, slow clearance from the body and hepatotoxicity).[3-5] To overcome these limitations, there is a need for the development of new classes of PSs. Among others, the use of transition metal complexes[6-11] and especially, Ru(II) polypyridine complexes are gaining momentum due to their attractive photophysical and chemical properties (i.e., strong luminescence, high singlet oxygen production, high chemical and photophysical stability),[12-22] with the compound TLD-1433 having just entered phase II clinical trials for the treatment of non-muscle invasive bladder cancer.[23-25] Despite these remarkable properties, the vast majority of Ru(II) polypyridine complexes are excited using either blue or UV-A light. As the light tissue penetration depth is rather poor at these wavelengths, the application of these compounds to treat deep-seated or large tumors is limited.[26-30] To circumvent this drawback, there is a need for the development of PSs with an absorption towards the biological spectral window (600-900 nm), which can be achieved by a red shifted one photon (1P) absorption or the use of two photon (2P) absorption for 2P PDT, a technique that is not employed yet in the clinics. However, the ability of Ru(II) polypyridine complexes to absorb 2P simultaneously, expressed as the 2P cross section, remains relatively poor (~ 40-250 Goeppert-Mayer (GM)), limiting their applications in this field of research.[31-37]

To tackle these drawbacks, herein, we report a novel approach to design Ru(II) polypyridine complexes with a red shifted 1P and exceptionally strong of 2P absorption using an *in silico* optimization. The resulting compounds were synthesized, characterized and photophysically and biologically evaluated in-depth. Strikingly, while being able to overcome the limitations of clinically applied PS, the compounds were found to be phototoxic in various 2D monolayer cells, 3D multicellular tumor spheroids as well as to eradicate a multiresistant tumor inside a mouse model upon clinically relevant 1P and 2P excitation.

RESULTS AND DISCUSSION

With the aim of enhancing the absorption properties of Ru(2,2′-bipyridine)$_3$ without deterioration of its 1P absorption properties, the bipyridine ligand was functionalized with rigid π conjugated substituents acting as electron donating groups. This is expected to induce a 1P absorption red-shift towards the biological spectral window by intercalation of donor centered orbitals in the Ru centered frontier orbitals manifold (allowing transitions of metal-to-ligand charge transfer (MLCT) and ligand-to-metal charge transfer (LMCT) character at low energy). As *trans*-stilbene are highly effective 2P dyes[38], it would be of high interest to extend the ligand scaffold with such a moiety as well as to include terminal donor groups, namely (*E*,*E*')-4,4′-bisstyryl-2,2′-bipyridine (L-H), (*E,E'*)-4,4′-bis[*p*-(*N*,*N*-dimethylamino)styryl]-2,2′-bipyridine (L-NMe$_2$) and (*E,E'*)-4,4′-bis[*p*-methoxystyryl]-2,2′-bipyridine (L-OMe). The predicted spectra for the resulting complexes of L-H and the L-OMe series (Fig. S1) allow to evidence the presence of two main bands in the 400-600 nm region, stemming both from MLCT/LMCT type transitions but also from ligand centered (LC) charge transfer excitations. Detailed analysis of the 1P and of the lowest lying 2P computed data (Table S1-S4) indicated that the most intense lowest lying 2P absorption processes are associated with ligand centered CT transitions with an average CT distance of 2.9 to 6.3 Å. Overall, the computed data suggests that Ru(II) coordinated

(*E*,*E*')-4,4′-bisstyryl-2,2′-bipyridine complexes with donor substituents have a red shifted 1P and a strong 2P absorption.

Before the synthesis of the final compounds, the known experimental procedures to obtain the corresponding ligands were optimized[39-42] to a one-step high-yielding synthesis using mild conditions (Scheme S1). Having the ligands in hand, the desired complexes **1-7** were synthesized. All compounds were analyzed by ^{1}H, ^{13}C-NMR, ESI-HRMS (Scheme S2-S3, Fig. S2-S22) and their purity confirmed by HPLC as well as elemental analysis. Additionally, the ligands L-H, L-NMe_2 and L-OMe as well as **3** were characterized using single crystal X-ray crystallography (Table S5-S6, Fig. S23-S26). Details on the synthesis and characterization can be found in the SI.

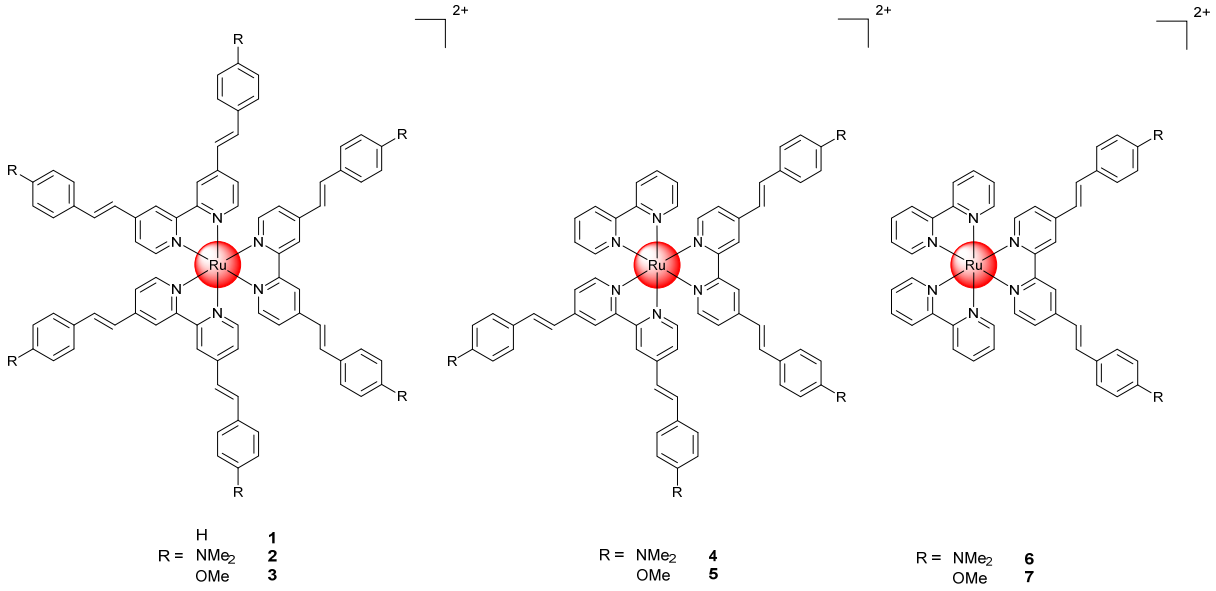

Fig. 1. Chemical structures of complexes **1-7** investigated in this study. The complexes were isolated as PF_6^- salts.

The photophysical properties of the complexes (Table S7-S8, Fig. S27) were then experimentally investigated to evaluate their potential as PDT PSs. In agreement with theoretical findings, the compounds generally show a red-shift of the first 1P absorption (Fig.

2a) band maximum of about 50-70 nm for the symmetric Ru(II) complexes in comparison to $Ru(bipy)_3$[43] as well as an absorption tail towards the near-infrared region. Strikingly and in agreement with theoretical data, the reported compounds have an exceptionally strong 2P absorption (Fig. 2b) with values up to ~6800 GM, which is an order of magnitude higher than the ones reported before for other Ru(II) polypyridine complexes.[31-37] Interestingly, the L-NMe_2 coordinated complexes were found with larger σ_2 values than the L-OMe and L-H coordinated compounds. Overall, the compounds have a 1P absorption tail towards and a strong 2P absorption in the biological spectral window, potentially allowing for the treatment of deep-seated or large tumors.

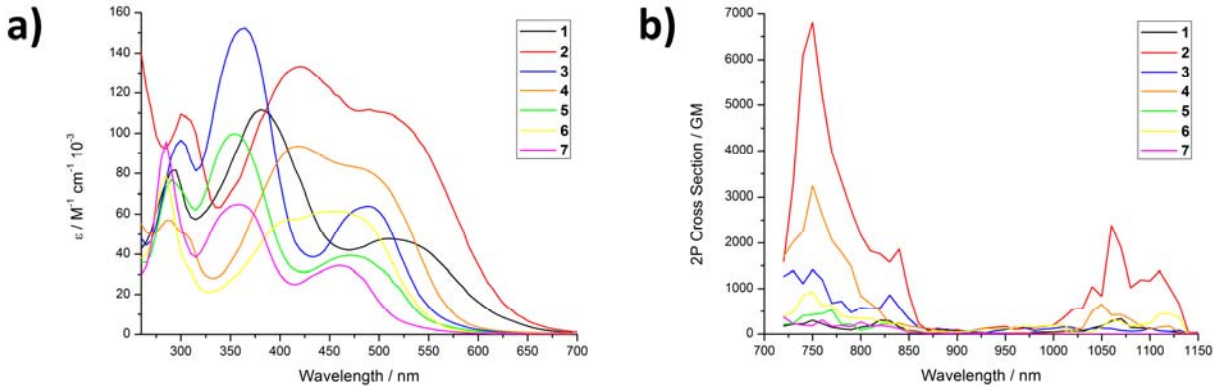

Fig. 2. a) 1P and **b)** 2P absorption spectra of the complexes **1**-**7**.

The luminescence quantum yields of the L-OMe coordinated complexes (**3**: 1.1%, **5**: 1.4%, **7**: 2.8%) were found to be significantly higher than those of the L-H coordinated (**1**: 1.9%) or L-NMe_2 coordinated (**2**: >0.1%, **4**: 0.4%, **6**: 0.5%) compounds. All complexes were found to have excited state lifetimes in the nanosecond range (Fig. S28-S34) in degassed (222-542 ns) and aerated saturated (36-96 ns) solutions. As the lifetimes drastically decrease in the presence of air, it indicates that the excited state can interact with an air component. For identification of the type of ROS produced upon light exposure, electron spin resonance spectroscopy was employed using the singlet oxygen ($^1O_2$) scavenger 2,2,6,6–tetramethylpiperidine and the $^{\bullet}OOH$ or $^{\bullet}OH$ radical scavenger 5,5-dimethyl-1-pyrroline *N*-oxide. While no signals for the formation

of •OOH or •OH radicals were detected, the formation of $^1O_2$ in CH_3CN and PBS was confirmed by observation of the characteristic $^1O_2$ -induced triplet signal in the ESR spectrum (Fig. S35-S41). The amount of generated $^1O_2$ was quantitatively determined by two methods: directly by measurement of the phosphorescence of $^1O_2$; indirectly by monitoring the change in absorbance of a $^1O_2$ scavenger. The singlet oxygen quantum yields were found to be between 16-77% in CH_3CN and 1-11% in an aqueous solution (Table S9). The comparison between the values indicates that the L-OMe coordinated complexes (**3**, **5**, **7**) are able to produce $^1O_2$ more efficiently than **1** and the L-NMe_2 coordinated Ru(II) complexes (**2**, **4**, **6**). Overall, complex **7** was found with the highest singlet oxygen quantum yield (CH_3CN: 68-77%, aqueous solution: 10-11%).

The stability of the compounds was investigated by incubation in human plasma at 37 °C for 48 h. The comparison of the HPLC chromatograms (Fig. S42-S48) showed no change before and after incubation in human plasma for all compounds, indicative of the stability of the complexes under biological conditions. Additionally, the stability upon irradiation was investigated (Fig. S49-S57) as the majority of currently clinically employed PSs suffer from this drawback. Importantly, no significant differences in the absorption spectra for the **L-OMe** coordinated complexes (**3**, **5**, **7**) and **1** were observed over time, indicating their photostability. On the contrary, small changes in the absorption spectra of the **L-NMe_2** coordinated complexes (**2**, **4**, **6**), especially of **2**, were observed, suggesting that the complexes are slightly photobleaching. Worthy of note, under identical experimental conditions, the absorption spectra of the known PS Protoporphyrin IX (PpIX) was found to be drastically changed, indicating a significantly stronger photobleaching. The study of the effect of the irradiation on the molecular structure of **2** by NMR spectroscopy suggests the decomposition of the compound (Fig. S58).

All compounds were found to be lipophilic with high distribution coefficients between an organic octanol and an aqueous PBS phase (Table S10). The time-dependent cellular uptake of

the complexes was then investigated in human cervical carcinoma (HeLa) cells by determining the amount of Ru inside the cells by inductively coupled plasma mass spectrometry (ICP-MS) at each time point. The results show that the asymptotic maximum (Fig. S59-S65) of the uptake of the compounds was reached within 8 h. As expected, the compounds with a higher lipophilicity, except of **2**, were found to have the highest uptake (Fig. S66). The uptake mechanism of the complexes was then investigated by blocking various pathways by preincubation with a cationic transporter (tetraethylammonium chloride), metabolic (2-deoxy-*D*-glucose and oligomycin) and endocytotic inhibitors (ammonium chloride or chloroquine) as well as at reduced temperature (4° C). Since all compounds were found with a similar profile (Fig. S67-S73), it suggests that these are internalized by the same mechanism, namely an energy-dependent endocytosis pathway. The localization of the complexes in HeLa cells was then investigated by confocal laser scanning microscopy. The distribution pattern of the luminescence of the compounds by 1P- (Fig. S74) and 2P- (Fig. S75) excitation was compared with the ones of commercial dyes for major cellular organelles (i.e., nucleus, mitochondria, lysosomes, golgi apparatus, endoplasmic reticulum). As no significant congruency was detected, it suggests that the complexes do not majorly localize in these organelles. In addition, the cellular localization was also investigated by separately extracting the cellular organelles (i.e., cytoplasm, mitochondria, lysosome, nucleus) and determining the amount of Ru by ICP-MS. The results (Fig. S76) indicate that all complexes majorly localize in the cytoplasm with small amount of unselective accumulation.

After an assessment of the uptake and the generation of $^1O_2$ upon light exposure in a cuvette, the generation of ROS inside of HeLa cells upon 1P- (488 nm, Fig. S77) and 2P (800 nm, Fig. S78) excitation was confirmed using the probe 2′,7′-dichlorofluorescein diacetate. To study their efficiency as PDT PSs, their cytotoxicity in the dark as well as upon irradiation at 480 nm (10 min, 3.1 J/cm^2) and 540 nm (40 min, 9.5 J/cm^2) towards non-cancerous retinal pigment

epithelium (RPE-1), HeLa, mouse colon carcinoma (CT-26) and human glioblastoma astrocytoma (U373) cells was investigated. Importantly, all complexes were found to be non-toxic in the dark ($IC_{50,\ dark}$ >100 μM) in all cell lines (Table S11-S12). This is an important requirement for a PDT agent. As desired, all compounds were found to be phototoxic in the micromolar range ($IC_{50,\ 480\ nm}$ = 0.7 - 53.6 μM, $IC_{50,\ 540\ nm}$ = 0.9 - 83.1 μM) in the different cell lines employed in this study. As the lead compounds of this study, complex **7** had an IC_{50} value even in the nanomolar range in CT-26 cells ($IC_{50,\ dark}$ >100 μM, $IC_{50,\ 480\ nm}$ = 0.7 ± 0.4 μM, $IC_{50,\ 540\ nm}$ = 0.9 ± 0.3 μM) with a PI value > 143. Under identical experimental conditions, the anticancer drug cisplatin and the well-known PS PpIX display a magnitude lower (photo-)toxicity. The cell death mechanism of the complexes was then evaluated by measuring the cell viability upon preincubation with autophagy (3-methyladenine), apoptosis (Z-VAD-FMK), paraptosis (cycloheximide) and necrosis (necrostatin-1) inhibitors (Fig. S79). While apoptosis was found to be the cell death mechanism for **1**-**5**, **6**-**7** triggered cell death by a combination of apoptosis and paraptosis pathways.

After evaluation of the biological effects of the compounds on 2D monolayer cells, their ability to act on 3D multicellular tumor spheroids (MCTS) was investigated. MCTS simulate the conditions found in clinically treated tumors including hypoxia and proliferation gradients to the center.[44] Consequently, the penetration of the compounds inside of HeLa MCTS with a diameter of 800 μm was investigated by 1P and 2P z-stack confocal laser scanning microscopy. **4**-**7** completely penetrated the MCTS within 12 h with a strong luminescence signal at every section depth, whereas **1**-**3** were mostly found on the outer sphere (Fig. S80-S86). Upon an increased incubation time up to 60 h, the remaining compounds were also able to penetrate the MCTS, with exception to **2**, which was still found mostly on the outer sphere (Fig. S87-S91). Following this, the tumor growth inhibition effect of **1**-**7** (20 μM) in HeLa MCTS was investigated and compared to the well-known PS tetraphenylporphyrin (H_2TPP) (20 μM) and

cisplatin (10 µM, 30 µM). The compounds were incubated for 3 days in the dark as this time was shown to be required for a complete MCTS penetration. The MCTS were then exposed to a 1P (500 nm, 10 J/cm^2) or 2P irradiation (800 nm, 10 J/cm^2, section interval of 5 µm) on day 3. During the whole time period, the shape and volume of the MCTS was constantly monitored. As expected, the MCTS treated with **1**-**7** or H_2TPP in the dark (Fig. 3a, representative image of MCTS: Fig. S92) were asymptotically growing in the same manner than the control group, indicating that the compounds do not show any inhibitory effect whereas cisplatin showed a weak effect on the tumor growth. On the contrary, the volume of the MCTS treated with complexes **1**-**7** and exposed to 1P or 2P irradiation (Fig. 3b-3c, representative image of MCTS: Fig. S93-S94) significantly shrank, demonstrating their strong tumor inhibition effect.

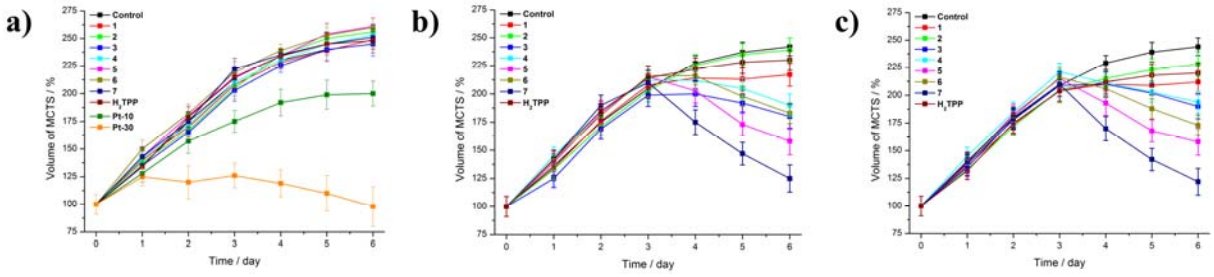

Fig. 3. Tumor growth inhibition assay. Change of the volume in HeLa MCTS in correlation to the time of the treatment. The MCTS were treated with compounds **1**-**7** (20 µM, 2% DMSO, *v*%), H_2TPP (20 µM, 2% DMSO, *v*%) and cisplatin (10 µM and 30 µM). The MCTS were **a)** strictly kept in the dark, **b)** exposed to 1P irradiation (500 nm, 10 J/cm^2), **c)** exposed to 2P irradiation (800 nm, 10 J/cm^2 with a section interval of 5 µm) on day 3. The error bars correspond to the standard deviation of the three replicates.

To further study the effect the complexes on the tumor survival, the treated MCTS were stained with a cellular living cell kit using Calcein AM (Fig. 4). The fluorescence images confirmed

that the MCTS treated with **1**-**7** in the dark and with **1**-**3** upon a 1P irradiation (500 nm, 10 J/cm^2) or 2P irradiation (800 nm, 10 J/cm^2, section interval of 5 μm) are still intact. The low phototoxic effect of **1**-**3** is caused by the poor MCTS penetration. Promisingly, the MCTS treated with **4**-**7** and exposed to 1P or 2P light were completely eradicated.

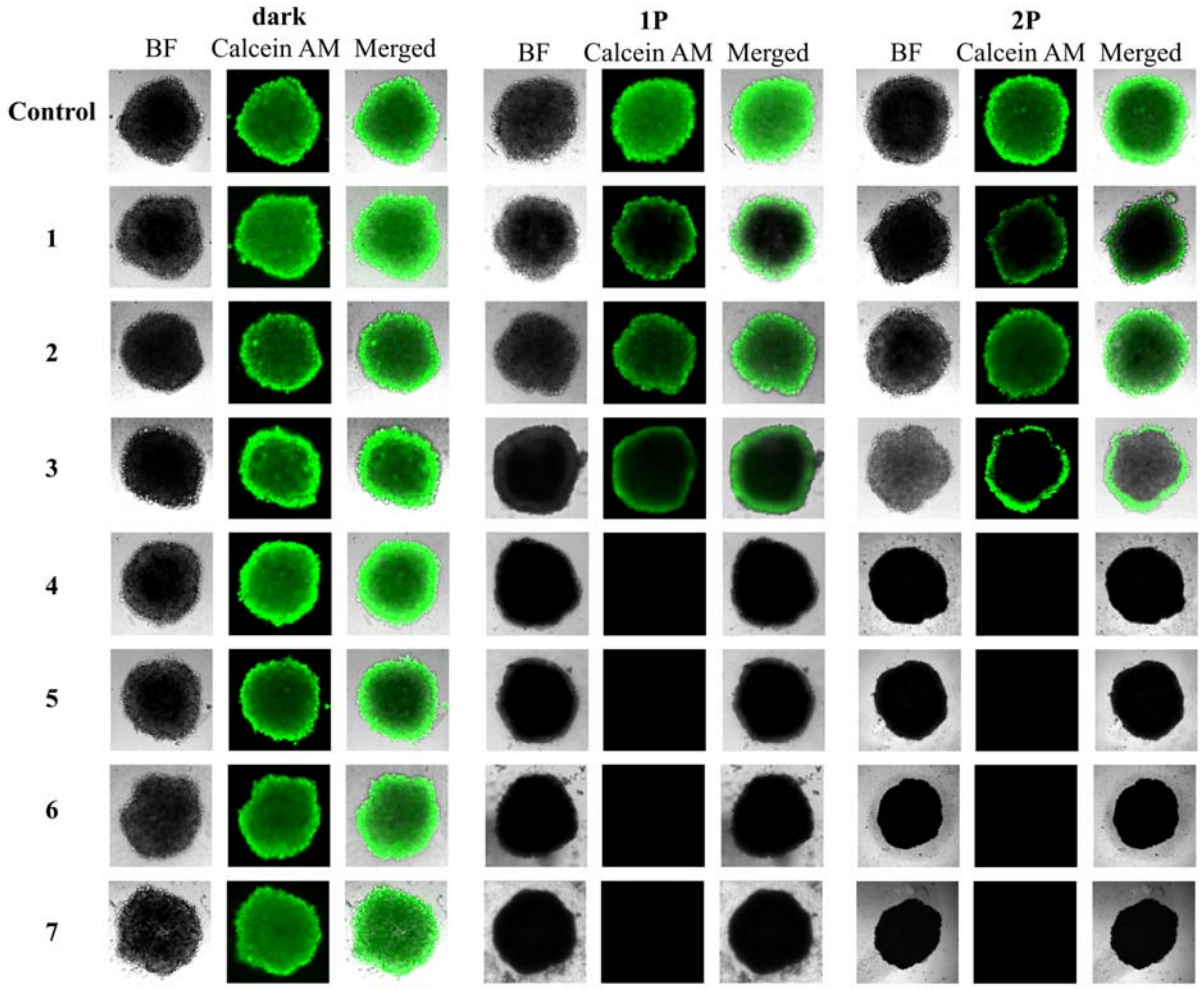

Fig. 4. Representative image of a viability assay in HeLa MCTS. MCTS were treated with compounds **1**-**7** (20 μM, 2% DMSO, *v*%) in the dark for three days. After this time, MCTS were kept in the dark, exposed to 1P irradiation (500 nm, 10 J/cm^2) or to 2P irradiation (800 nm, 10 J/cm^2, section interval of 5 μm). After two days, the cell viability was assessed by measurement of the fluorescence of calcein (λ_{ex} = 495 nm, λ_{em} = 515 nm), which is generated in living cells from calcein AM.

The photodynamic effect using a 1P (500 nm, 10 J/cm^2) and 2P irradiation (800 nm, 10 J/cm^2, section interval of 5 µm) was then quantified by determination of the ATP concentration (Table S13). Importantly, no measurable cytotoxicity in the dark could be observed in HeLa MCTS for all compounds and **1**-**3** upon light exposure in agreement with the previous investigations. **4**-**6** were found to be phototoxic in the micromolar range ($IC_{50,\ 500\ nm}$ = 6.8 – 78.3 µM, $IC_{50,\ 800\ nm}$ = 1.4 – 87.3 µM). Strikingly, the lead compound of this study **7** was found to be non-toxic in the dark at even higher concentrations ($IC_{50,\ dark}$ > 300 µM), while being highly phototoxicity in the low micromolar range ($IC_{50,\ 500\ nm}$ > 6.8 ± 0.2 µM, $IC_{50,\ 800\ nm}$ > 1.4 ± 0.2) with exceptionally high PI values ($PI_{500\ nm}$ > 44, $PI_{800\ nm}$ > 250). Importantly, under identical experimental conditions, treatment with H_2TPP did not show a cytotoxic effect ($IC_{50,\ dark}$ = $IC_{50,\ 500\ nm}$ = $IC_{50,\ 800\ nm}$ > 100 µM), indicating that **7** is able to act at low drug and light doses compared to a clinically utilized tetrapyrrolic compound.

Capitalizing on these promising results, the biological properties of **7** to act as a PDT PS were further investigated in a mouse model. To ensure solubility and biocompatibility, the PS was converted to a Cl^- salt using a counter ion exchange resin. A challenging to treat multiresistant doxorubicin-selected P-gp-overexpressing human colon cancer tumor model (SW620/AD300) was used to evaluate the PS potential. The biodistribution of **7** (2 mg/Kg) inside this mouse model was then time-dependently (30 min, 1 h, 2 h) studied by intravenous tail-injection into nude mice. After each time point, the mice were sacrificed and the major organs (i.e., blood, spleen, intestine, stomach, liver, kidney, uterus, lung, heart, brain, tumor) were separated, grinded and the Ru content determined by ICP-MS. Interestingly, **7** was absorbed from the blood stream within 1 h with a high accumulation in the intestine and some accumulation in the tumor (Fig. S95). Following this, 1 h after an intravenous tail-injection of **7** (2 mg/Kg), *in vivo* PDT experiments using a 1P (500 nm, 10 mW/cm^2, 60 min) or 2P irradiation (800 nm, 50 mW, 1 kHz, pulse width 35 fs, 5 s/mm) were performed on mice with an 80 mm^3 tumor.

Encouragingly, after only one PDT treatment, the tumor drastically shrank until they were nearly eradicated whereas the tumors treated with the light or **7** in the dark (Fig. 5a, 5c) kept growing. Importantly, the animals treated with the compound behave normally, without signs of pain, stress or discomfort and did not lose or gain weight (Fig. 5b). After the treatment, the mice were sacrificed, the tumor and organs were separated and histologically examined by an H&E stain. The tumor tissue treated with **7** and exposed to light displayed pathological alterations caused by the PDT treatment (Fig. S96) while all other organs did not show any significant effect (Fig. S97). Overall, this study demonstrates the enormous potential of **7** as a PS for 1P and 2P PDT.

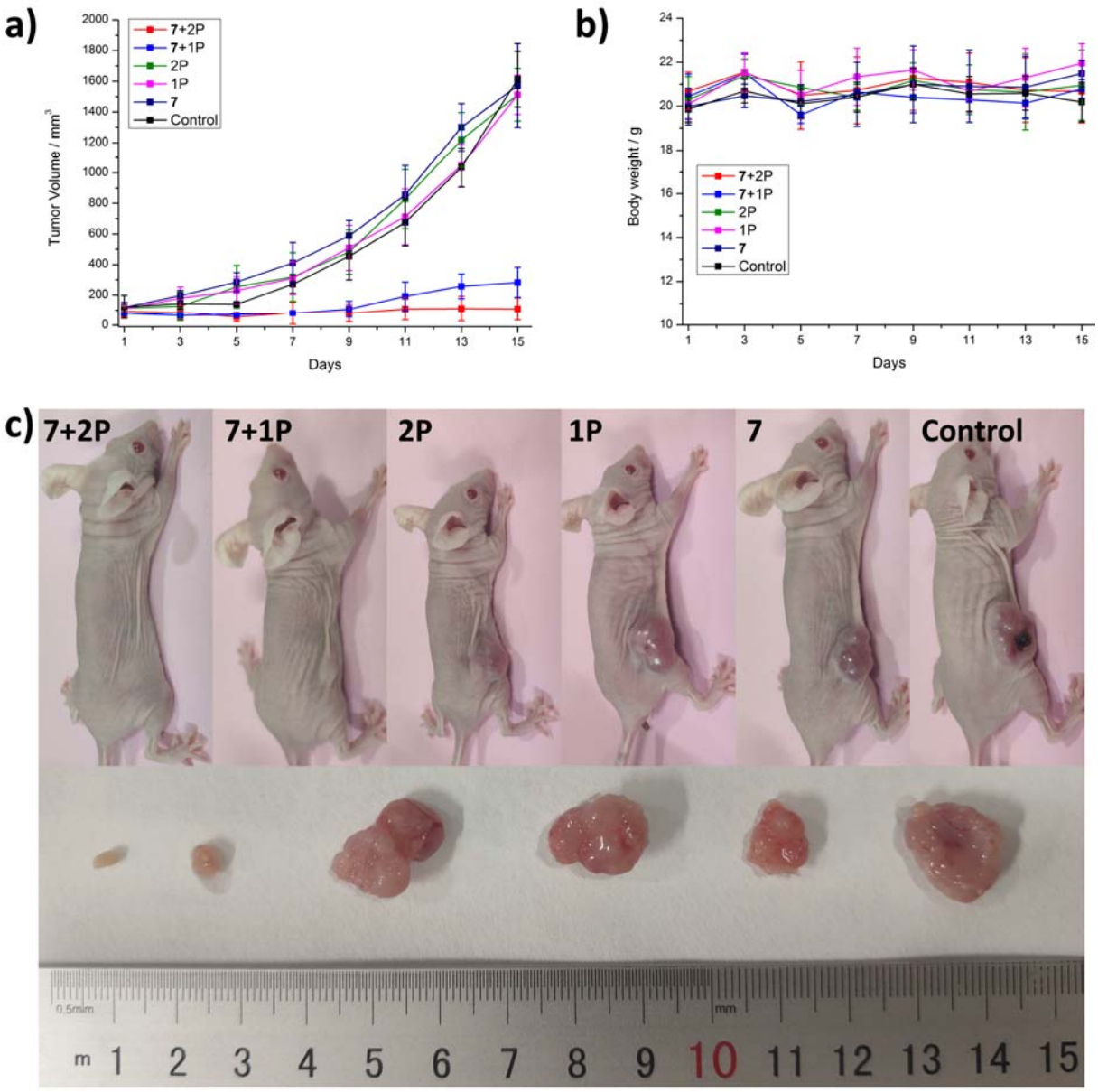

Fig. 5. *In vivo* PDT study of **7** using 1P (500 nm, 10 mW/cm^2, 60 min) or 2P (800 nm, 50 mW, 1 kHz, pulse width 35 fs, 5 s/mm) excitation on nude mice bearing a doxorubicin-selected P-gp-overexpressing human colon cancer tumor (SW620/AD300). **a)** Tumor growth inhibition curves upon treatment. **b)** Average body weights of the tumor-bearing mice. **c)** Representative photographs of the tumor-bearing mice.

CONCLUSION

Ru(II) polypyridine complexes with (*E*,*E*')-4,4′-bisstyryl-2,2′-bipyridine ligands have been rationally designed using DFT calculations and were found to have a remarkable red-shifted 1P absorption as well as exceptionally high 2P cross sections. The complexes were found to be taken up by cancerous cells through an energy-dependent endocytosis pathway and to majorly accumulate in the cytoplasm. Upon irradiation, they were found to generate $^1O_2$, causing a phototoxic effect by apoptosis and paraptosis pathways in various monolayer cells as well as multicellular tumor spheroids. *In vivo* studies confirmed the impressive ability of **7** to act as a PS upon treatment at clinically relevant 1P (500 nm) and 2P (800 nm) irradiation with an eradication of the tumor. Importantly, these compounds were found to be highly water soluble, stable in human plasma as well as upon constant irradiation and therefore are able to overcome the limitations of currently employed PSs. We strongly believe that these complexes have great potential for preclinical trials.

Acknowledgements

We thank Dr. Philippe Goldner for access to state-of-the-art laser apparatus. This work was financially supported by an ERC Consolidator Grant PhotoMedMet to G.G. (GA 681679), has received support under the program "Investissements d' Avenir" launched by the French Government and implemented by the ANR with the reference ANR-10-IDEX-0001-02 PSL (G.G.), the National Science Foundation of China (Nos. 21525105 and 21778079 for H.C.) and the 973 Program (No. 2015CB856301 for H.C.). I.C and F.M were financially supported from the European Research Council (ERC) under the European Union's Horizon 2020 research and innovation programme (grant agreement No 648558, STRIGES CoG grant).

Author Contributions

All authors were involved with the design and interpretation of experiments and with the writing of the manuscript. DFT calculations were performed by J.K. and F.M. Chemical, photophysical and biological experiments were carried out by J.K. X-ray crystallography was carried out by J.K. and O.B. Animal testing was carried out by J.K. and S. K. All authors have given approval to the final version of the manuscript.

Competing interests

The authors declare no competing financial interests.

Additional information

Supplementary Information is available with the online version of this paper. Correspondence and requests for materials should be addressed to H.C. or G.G.

REFERENCES

1. Bonnett, R. Photosensitizers of the porphyrin and phthalocyanine series for photodynamic therapy. *Chem. Soc. Rev.* **24**, 19-33 (1995).
2. Castano, A. P., Mroz, P. & Hamblin, M. R. Photodynamic therapy and anti-tumour immunity. *Nat. Rev. Cancer* **6**, 535-545 (2006).
3. Dolmans, D. E., Fukumura, D. & Jain, R. K. Photodynamic therapy for cancer. *Nat. Rev. Cancer* **3**, 380-387 (2003).

4. O'Connor, A. E., Gallagher, W. M. & Byrne, A. T. Porphyrin and nonporphyrin photosensitizers in oncology: Preclinical and clinical advances in photodynamic therapy. *Photochem. Photobiol.* **85**, 1053-1074 (2009).

5. Karges, J., Basu, U., Blacque, O., Chao, H. & Gasser, G. Polymeric Encapsulation of Novel Homoleptic Bis(dipyrrinato) Zinc(II) Complexes with Long Lifetimes for Applications as Photodynamic Therapy Photosensitisers. *Angew. Chem. Int. Ed.* **58**, 14334-14340 (2019).

6. Lo, K. K.-W. Luminescent Rhenium(I) and Iridium(III) Polypyridine Complexes as Biological Probes, Imaging Reagents, and Photocytotoxic Agents. *Acc. Chem. Res.* **48**, 2985-2995 (2015).

7. Huang, H., Banerjee, S., Qiu, K., Zhang, P., Blacque, O., Malcomson, T., Paterson, M. J., Clarkson, G. J., Staniforth, M., Stavros, V. G., Gasser, G., Chao, H. & Sadler, P. J. Targeted photoredox catalysis in cancer cells. *Nat. Chem.* **11**, 1041-1048 (2019).

8. McKenzie, L. K., Bryant, H. E. & Weinstein, J. A. Transition metal complexes as photosensitisers in one-and two-photon photodynamic therapy. *Coord. Chem. Rev.* **379**, 2-29 (2019).

9. Bruijnincx, P. C. & Sadler, P. J., New trends for metal complexes with anticancer activity. *Curr. Opin. Chem. Biol.* **12**, 197-206 (2008).

10. Novohradsky, V., Rovira, A., Hally, C., Galindo, A., Vigueras, G., Gandioso, A., Svitelova, M., Bresolí-Obach, R., Kostrhunova, H., Markova, L., Kasparkova, J., Nonell, S., Ruiz, J., Brabec, V. & Marchán, V. Towards Novel Photodynamic Anticancer Agents Generating Superoxide Anion Radicals: A Cyclometalated Ir^{III} Complex Conjugated to a Far-Red Emitting Coumarin. *Angew. Chem. Int. Ed.* **58**, 6311-6315 (2019).

11. Zamora, A., Vigueras, G., Rodríguez, V., Santana, M. D. & Ruiz, J., Cyclometalated iridium(III) luminescent complexes in therapy and phototherapy. *Coord. Chem. Rev.* **360**, 34-76 (2018).

12. Knoll, J. D. & Turro, C. Control and utilization of ruthenium and rhodium metal complex excited states for photoactivated cancer therapy. *Coord. Chem. Rev.* **282-283**, 110-126 (2015).

13. Liu, J., Zhang, C., Rees, T. W., Ke, L., Ji, L. & Chao, H. Harnessing ruthenium (II) as photodynamic agents: Encouraging advances in cancer therapy. *Coord. Chem. Rev.* **363**, 17-28 (2018).

14. Poynton, F. E., Bright, S. A., Blasco, S., Williams, D. C., Kelly, J. M. & Gunnlaugsson, T. The development of ruthenium(II) polypyridyl complexes and conjugates for in vitro cellular and in vivo applications. *Chem. Soc. Rev.* **46**, 7706-7756 (2017).

15. Howerton, B. S., Heidary, D. K. & Glazer, E. C. Strained Ruthenium Complexes Are Potent Light-Activated Anticancer Agents. *J. Am. Chem. Soc.* **134**, 8324-8327 (2012).

16. Lameijer, L. N., Ernst, D., Hopkins, S. L., Meijer, M. S., Askes, S. H. C., Le Dévédec, S. E. & Bonnet, S. A Red-Light-Activated Ruthenium-Caged NAMPT Inhibitor Remains Phototoxic in Hypoxic Cancer Cells. *Angew. Chem. Int. Ed.* **56**, 11549-11553 (2017).

17. Lincoln, R., Kohler, L., Monro, S., Yin, H., Stephenson, M., Zong, R., Chouai, A., Dorsey, C., Hennigar, R., Thummel, R. P. & McFarland, S. A. Exploitation of Long-Lived ^{3}IL Excited States for Metal–Organic Photodynamic Therapy: Verification in a Metastatic Melanoma Model. *J. Am. Chem. Soc.* **135**, 17161-17175 (2013).

18. Zeng, L., Gupta, P., Chen, Y., Wang, E., Ji, L., Chao, H. & Chen, Z.-S. The development of anticancer ruthenium (II) complexes: from single molecule compounds to nanomaterials. *Chem. Soc. Rev.* **46**, 5771-5804 (2017).

19. Li, A., Turro, C. & Kodanko, J. J. Ru (II) Polypyridyl Complexes Derived from Tetradentate Ancillary Ligands for Effective Photocaging. *Acc. Chem. Res.* **51**, 1415-1421 (2018).

20. Li, A., Turro, C. & Kodanko, J. J. Ru(II) polypyridyl complexes as photocages for bioactive compounds containing nitriles and aromatic heterocycles. *Chem. Commun.* **54**, 1280-1290 (2018).

21. Shum, J., Leung, P. K.-K. & Lo, K. K.-W. Luminescent Ruthenium(II) Polypyridine Complexes for a Wide Variety of Biomolecular and Cellular Applications. *Inorg. Chem.* **58**, 2231-2247 (2019).

22. Bonnet, S. & Collin, J.-P. Ruthenium-based light-driven molecular machine prototypes: synthesis and properties. *Chem. Soc. Rev.* **37**, 1207-1217 (2008).

23. Shi, G., Monro, S., Hennigar, R., Colpitts, J., Fong, J., Kasimova, K., Yin, H., DeCoste, R., Spencer, C., Chamberlain, L., Mandel, A., Lilge, L. & McFarland, S. A. Ru(II) dyads derived from α-oligothiophenes: A new class of potent and versatile photosensitizers for PDT. *Coord. Chem. Rev.* **282-283**, 127-138 (2015).

24. Monro, S., Colón, K. L., Yin, H., Roque III, J., Konda, P., Gujar, S., Thummel, R. P., Lilge, L., Cameron, C. G. & McFarland, S. A. Transition Metal Complexes and Photodynamic Therapy from a Tumor-Centered Approach: Challenges, Opportunities, and Highlights from the Development of TLD1433. *Chem. Rev.* **119**, 797-828 (2019).

25. McFarland, S. A., Mandel, A., Dumoulin-White, R. & Gasser, G. Metal-based photosensitizers for photodynamic therapy: the future of multimodal oncology? *Curr. Opin. Chem. Biol.* **56**, 23-27 (2020).

26. Heinemann, F., Karges, J. & Gasser, G. Critical Overview of the Use of Ru (II) Polypyridyl Complexes as Photosensitizers in One-Photon and Two-Photon Photodynamic Therapy. *Acc. Chem. Res.* **50**, 2727-2736 (2017).

27. Wachter, E., Heidary, D. K., Howerton, B. S., Parkin, S. & Glazer, E. C. Light-activated ruthenium complexes photobind DNA and are cytotoxic in the photodynamic therapy window. *Chem. Commun.* **48**, 9649-9651 (2012).

28. Karges, J., Heinemann, F., Maschietto, F., Jakubaszek, M., Subecz, C., Dotou, M., Blacque, O., Tharaud, M., Goud, B., Zahínos, E. V., Spingler, B., Ciofini, I., Gasser, G. Rationally Designed Long-Wavelength Absorbing Ru(II) Polypyridyl Complexes as Photosensitizers for Photodynamic Therapy. Preprint at https://doi.org/10.26434/chemrxiv.11336669.v1 (2019).

29. Karges, J., Blacque, O., Goldner, P., Chao, H. & Gasser, G. Towards Long Wavelength Absorbing Photodynamic Therapy Photosensitizers via the Extension of a $[Ru(bipy)_3]^{2+}$ Core. *Eur. J. Inorg. Chem.* **2019**, 3704-3712 (2019).

30. Idris, N. M., Gnanasammandhan, M. K., Zhang, J., Ho, P. C., Mahendran, R. & Zhang Y. *In vivo* photodynamic therapy using upconversion nanoparticles as remote-controlled nanotransducers. *Nat. Med.* **18**, 1580-1585 (2012).

31. Boca, S. C., Four, M., Bonne, A., Van Der Sanden, B., Astilean, S., Baldeck, P. L. & Lemercier, G. An ethylene-glycol decorated ruthenium (II) complex for two-photon photodynamic therapy. *Chem. Commun.* 4590-4592 (2009).

32. Girardot, C., Lemercier, G., Mulatier, J. C., Chauvin, J., Baldeck, P. L. & Andraud, C. Novel ruthenium(II) and zinc(II) complexes for two-photon absorption related applications. *Dalton Trans.* 3421-3426 (2007).

33. Liu, J., Chen, Y., Li, G., Zhang, P., Jin, C., Zeng, L., Ji, L. & Chao, H. Ruthenium (II) polypyridyl complexes as mitochondria-targeted two-photon photodynamic anticancer agents. *Biomaterials* **56**, 140-153 (2015).

34. Zeng, L., Kuang, S., Li, G., Jin, C., Ji, L. & Chao, H. A GSH-activatable ruthenium(II)-azo photosensitizer for two-photon photodynamic therapy. *Chem. Commun.* **53**, 1977-1980 (2017).

35. Qiu, K., Wang, J., Song, C., Wang, L., Zhu, H., Huang, H., Huang, J., Wang, H., Ji, L. & Chao, H. Crossfire for Two-Photon Photodynamic Therapy with Fluorinated Ruthenium (II) Photosensitizers. *ACS Appl. Mater. Interfaces* **9**, 18482-18492 (2017).

36. Huang, H., Yu, B., Zhang, P., Huang, J., Chen, Y., Gasser, G., Ji, L. & Chao, H. Highly Charged Ruthenium (II) Polypyridyl Complexes as Lysosome-Localized Photosensitizers for Two-Photon Photodynamic Therapy. *Angew. Chem. Int. Ed.* **54**, 14049-14052 (2015).

37. Hess, J., Huang, H., Kaiser, A., Pierroz, V., Blacque, O., Chao, H. & Gasser, G. Evaluation of the Medicinal Potential of Two Ruthenium (II) Polypyridine Complexes as One-and Two-Photon Photodynamic Therapy Photosensitizers. *Chem. Eur. J.* **23**, 9888-9896 (2017).

38. Pawlicki, M., Collins, H. A., Denning, R. G. & Anderson, H. L. Two-Photon Absorption and the Design of Two-Photon Dyes. *Angew. Chem. Int. Ed.* **48**, 3244-3266 (2009).

39. Bourgault, M., Renouard, T., Lognoné, B., Mountassir, C. & Bozec, H. L. Synthesis and characterization of 4-alkenyl and 4, 4′-dialkenyl-2, 2′-bipyridyl ligands bearing π-donor substituents. *Can. J. Chem.* **75**, 318-325 (1997).

40. Juris, A., Campagna, S., Bidd, I., Lehn, J. M. & Ziessel, R. Synthesis and photophysical and electrochemical properties of new halotricarbonyl (polypyridine) rhenium (I) complexes. *Inorg. Chem.* **27**, 4007-4011 (1988).

41. Balasubramanian, K., Cammarata, V. & Wu, Q. Langmuir-Schaefer films: head group influence on orientation of substituted styryl bipyridines. *Langmuir* **11**, 1658-1665 (1995).

42. Leidner, C., Sullivan, B. P., Reed, R., White, B., Crimmins, M., Murray, R. W. & Meyer, T. J. Synthesis and electropolymerization of distyrylbipyridine and methyldistyrylbipyridine complexes of iron, ruthenium, osmium, rhenium, and cobalt. *Inorg. Chem.* **26**, 882-891 (1987).

43. Karges, J., Heinemann, F., Maschietto, F., Patra, M., Blacque, O., Ciofini, I., Spingler, B. & Gasser, G. A Ru(II) polypyridyl complex bearing aldehyde functions as a versatile synthetic precursor for long-wavelength absorbing photodynamic therapy photosensitizers. *Biorg. Med. Chem.* **27**, 2666-2675 (2019).

44. Friedrich, J., Seidel, C., Ebner, R. & Kunz-Schughart, L. A. Spheroid-based drug screen: considerations and practical approach. *Nat. Protoc.* **4**, 309-324 (2009).

Table of Contents Graphic: